

Dirac Wave Functions in Nuclear Distorted-Wave Calculations

E. Rost, J. R. Shepard, and D. Murdock

Nuclear Physics Laboratory, University of Colorado, Boulder, Colorado 80309

(Received 22 April 1982)

A distorted-wave formulation of simple direct nuclear reactions, using Dirac wave functions, is presented. The resulting amplitude contains interior damping due to relativistic Darwin terms. The calculations are compared with standard Schrödinger results and significant differences are found.

PACS numbers: 24.10.Fr, 25.40.Ep, 25.40.Gr

During the past few years an optical model for nucleon-nucleus elastic scattering based on the Dirac equation has been developed¹ as an alternative to the standard Schrödinger-equation formulation. The Dirac phenomenological potential consists of a mixture of Lorentz scalar and Lorentz vector parts which, in combination, provide the central and spin-orbit potentials of the nuclear optical model. Application² to proton elastic scattering explains some of the energy dependence and geometric anomalies obtained with conventional optical-model fits to data. In a recent paper, Cooper and Sherif³ have successfully calculated (p_{pol}, π^+) reaction observables with a distorted-wave Born-approximation (DWBA) approach using Dirac wave functions.

In this Letter we report the extension of the Dirac description to inelastic scattering and nucleon transfer reactions. Since the motivation is to assess the effect of Dirac wave functions, we consider only simple nuclear direct reactions where the transition amplitude is

$$T_{fi} = \int d^3r \chi_f^{(-)*}(\vec{k}_f, \vec{r}) O_{fi} \chi_i^{(+)}(\vec{k}_i, \vec{r}). \quad (1)$$

$$\left\{ -\frac{\nabla^2}{2E} + V_{\text{cen}}(r) + V_{\text{so}}(r) [\vec{\sigma} \cdot \vec{L} - \vec{r} \cdot \nabla] - \frac{(E^2 - m^2)}{2E} \right\} \psi = 0, \quad (3a)$$

$$V_{\text{cen}}(r) = V_v(r) + (m/E)V_s(r) + V_c(r) - (2E)^{-1} [V_v^2(r) - V_s^2(r) + 2V_v(r)V_c(r)], \quad (3b)$$

$$V_{\text{so}}(r) = (2EBr)^{-1} dB/dr, \quad (3c)$$

$$B(r) = 1 + [V_s(r) - V_v(r)]/(E + m). \quad (3d)$$

In Eqs. (3) small terms in $V_c^2(r)$ and $d/dr V_c(r)$ have been dropped so that ψ has the usual asymptotic form.

The term containing $\vec{r} \cdot \nabla$ is known as the Darwin term⁵ and may be transformed away by setting

$$\psi(\vec{r}) = B^{1/2}(r) \varphi(\vec{r}) \quad (4)$$

and substituting into Eq. (3). The resulting equation for $\varphi(\vec{r})$ becomes

$$\left\{ -\frac{\nabla^2}{2E} + U_{\text{eff}}(r) + V_{\text{so}}(r) \vec{\sigma} \cdot \vec{L} - \frac{(E^2 - m^2)}{2E} \right\} \varphi(\vec{r}) = 0 \quad (5)$$

Such a form is appropriate for the cases of non-exchange inelastic scattering [which includes (p, n) reactions] and nucleon pickup in the zero-range approximation. The χ 's are distorted waves and the local, nonrelativistic operator O_{fi} may contain one or more bound-state wave functions depending on the particular model employed.

In this work we consider the distorted continuum and bound-state wave functions to be the upper components of solutions to Dirac equations. For the nucleon problems, the Dirac equation reads ($\hbar = c = 1$)

$$\{ \vec{\alpha} \cdot \vec{p} + \beta [m + V_s(r)] + V_v(r) + V_c(r) - E \} \Psi = 0, \quad (2)$$

where *real* Dirac scalar, Dirac vector, and Coulomb potentials are added to the free Dirac Hamiltonian with total energy E . The mass m is taken to be the reduced total energy to account for recoil in a minimum relativistic manner.⁴ Standard manipulations now transform Eq. (2) into a second-order differential equation for the upper component ψ ,

with

$$U_{\text{eff}}(r) = V_{\text{cen}}(r) - \frac{1}{2Br^2} \frac{d}{dr} \left(r^2 \frac{dB}{dr} \right) + \frac{3}{4B^2} \left(\frac{dB}{dr} \right)^2 + iW(r), \quad (6)$$

where we have added an imaginary term $iW(r)$ to account for absorptive processes. This choice differs from previous work¹⁻³ where Dirac vector and scalar potentials were taken to be complex at the start. Our method has the advantage of avoiding creative potential terms and also allows for the convenience of using Schrödinger-equation phenomenology for initial imaginary starting values in optical-model searches. Equivalent elastic-scattering fits to data are obtainable with this approach; however, our main result (Darwin damping) occurs as well with alternative parametrizations of $W(r)$.

Deuteron-nucleus distorted waves are required for the pickup calculations. Extension of the Dirac phenomenology to deuteron scattering is the subject of another paper.⁶ One arrives at an equation of the same form similar to the above but with the following modifications:

$$V_{s.o.}^{(d)}(r) = \frac{-1}{2E_d r} \frac{dV_v^{(d)}/dr}{E_d - V_v^{(d)}}, \quad (7a)$$

$$B^{(d)}(r) = 1 + V_s^{(d)}(r)/m_d. \quad (7b)$$

The damping factor $B^{1/2}$ is comparable to that for a nucleon while the spin-orbit potential is about half as large as the nucleon case.⁵

The crucial feature for reaction analyses using Dirac wave functions is the presence of the damping factor $B^{1/2}(r)$ in Eq. (4). This factor is typically about 0.75 near the origin and rises to unity in the nuclear surface. Since this factor appears in bound-state wave functions as well as both distortion terms, it provides a significant damping of the nuclear interior in a reaction calculation. By contrast, the effect on elastic scattering occurs only in the extra terms in Eq. (6) which are small.¹ The surprisingly large damping due to the Darwin term is connected to the large spin-orbit interaction since both have the same multiplying factor $V_{s.o.}(r)$. This factor is ~ 25 times the Thomas relativistic effect and is therefore more important than other relativistic effects which are ignored.

All the ingredients of the DWBA are now specified given appropriate potentials V_s , V_v , and W and may be processed by reaction codes.⁷ The proton-nucleus potentials are determined by fitting to the relevant elastic scattering cross-section and analyzing-power data and the quality of

the fits are comparable to those shown in Ref. 2. The geometric parameters obtained are also used for the nucleon bound-state wave functions. For our deuteron wave function we use the Dirac formulation of Ref. 6 and construct a deuteron potential which is consistent with proton scattering data at half the incident deuteron kinetic energy. Such a potential then is a Dirac analog to a Johnson-Soper⁸ potential which is often appropriate for stripping and pickup calculations.

We now apply the Dirac wave functions to sample DWBA calculations and compare them with standard Schrödinger wave function calculations. Both cases involve $l=0$ transfer where the nuclear interior contributions are significant.

In Fig. 1, DWBA calculations are shown for the $^{90}\text{Zr}(p, n)^{90}\text{Nb}$ (isobaric analog state) transition at $T_p = 80$ MeV. The analysis employs a microscopic $(1g_{9/2})^2$ form factor with a central Yukawa effective interaction of range 1 fm. The continuum Dirac and Schrödinger potentials were determined by fitting to the proton elastic-scattering data of Schwandt *et al.*⁹ using the same imaginary potential in both cases. The bound-state $g_{9/2}$ nucleon wave functions were generated with use of the geometry of the real part of the scattering potential with depths adjusted to fit the $g_{9/2}$ nucleon separation energy in ^{90}Zr . It is clear from Fig. 1 that the use of Dirac wave

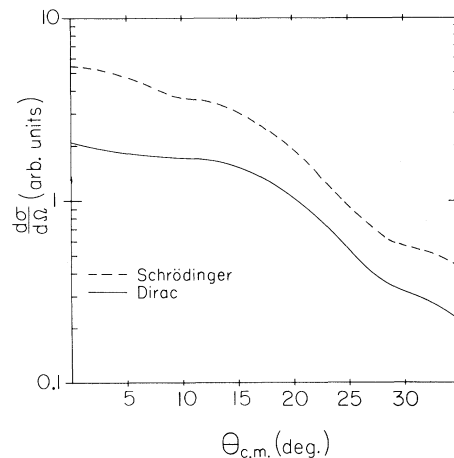


FIG. 1. Comparison of Schrödinger and Dirac calculations for the reaction $^{90}\text{Zr}(p, n)^{90}\text{Nb}$ (isobaric analog state) at $T_p = 80$ MeV.

functions causes an appreciable reduction in the (p, n) cross sections. This reduction is directly traced to the damping factor of the Darwin term and gives a factor of about 2 in this case. Distorted-wave damping alone will give almost the total effect.

A more extreme case is presented in Fig. 2 where DWBA calculations for the $^{24}\text{Mg}(p, d)^{23}\text{Mg}$

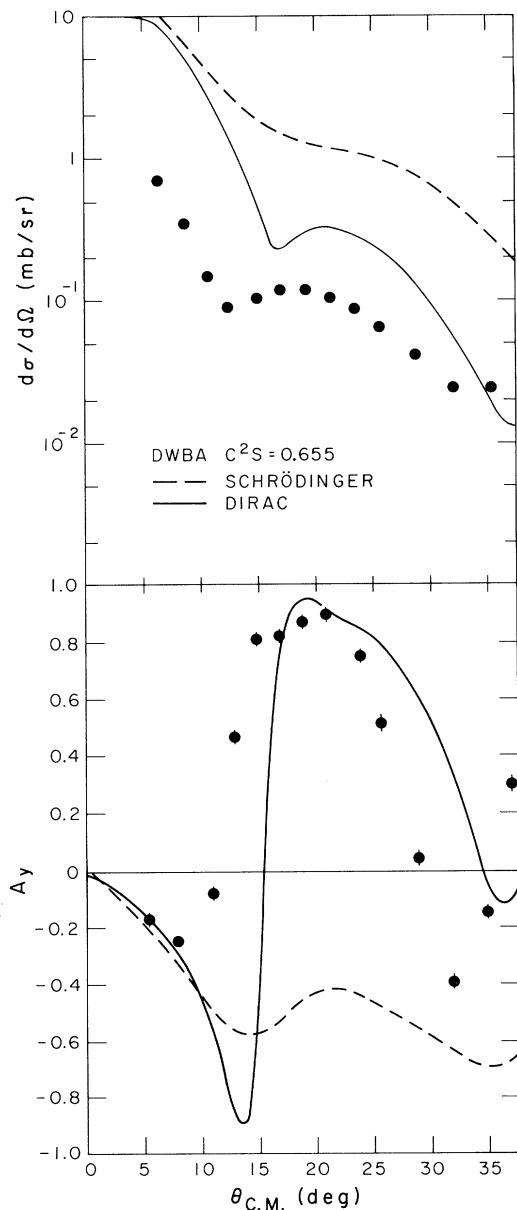


FIG. 2. Zero-range DWBA calculations for the reaction $^{24}\text{Mg}(p, d)^{23}\text{Mg}$ (2.36 MeV, $\frac{1}{2}^+$) at $T_p = 94$ MeV using Schrödinger and Dirac wave functions are compared with data.

(2.36 MeV, $\frac{1}{2}^+$) transition at $T_p = 94$ MeV are shown. Angular momentum transfer $l=0$ stripping calculations are notoriously sensitive to the reaction model especially in the analyzing powers. Despite this sensitivity an earlier work¹⁰ presented our failure to achieve even qualitative agreement between "conventional" DWBA calculations and experiment.¹¹ The Dirac calculations shown use proton potentials obtained by fitting the 99-MeV $p_{\text{pol}} + ^{28}\text{Si}$ data of Olmer *et al.*¹² and deuteron potentials constructed from 49.5-MeV $p_{\text{pol}} + ^{24}\text{Mg}$ data¹³ on ^{24}Mg . The Schrödinger calculations are taken from Ref. 10 and both calculations are normalized with the theoretical spectroscopic factor of Chung and Wildenthal as reported by Miller *et al.*¹⁴ Although the agreement with data in Fig. 2 is not perfect it represents a major improvement in the direction of qualitative agreement with experiment. This is a direct result of the nuclear interior suppression which is a *natural* consequence of using Dirac wave functions.

In summary, distorted-wave calculations with Dirac wave functions contain damping due to the relativistic Darwin term and this damping can affect magnitudes and shapes of the calculated cross sections and analyzing powers. The calculations we have presented contain several simplifying assumptions and, in addition, are inconsistent in that the interaction causing the transition is not treated in the Dirac framework. Also, small components of the wave functions are ignored. More work is needed to understand the importance of these approximations as well as to study the systematics of DWBA reaction analyses with Dirac wave functions. Previous reaction analyses have often employed artificial radial cutoffs to obtain agreement with data and it is plausible that many of these cases can now be explained using Dirac wave functions. Thus DWBA reaction analyses provide support for Dirac phenomenology in the interaction of nucleons with nuclei.

This work was supported in part by the U. S. Department of Energy.

¹L. B. Arnold, B. C. Clark, and R. L. Mercer, Phys. Rev. C **19**, 917 (1979), and references therein.

²L. B. Arnold, B. C. Clark, R. L. Mercer, and P. Schwandt, Phys. Rev. C **23**, 1949 (1981); L. G. Arnold *et al.*, Phys. Rev. C **25**, 936 (1982).

³E. D. Cooper and H. S. Sherif, Phys. Rev. Lett. **47**,

818 (1981).

⁴M. L. Goldberger and K. M. Watson, *Collision Theory* (Robert E. Kreuger, Huntington, N.Y., 1975).⁵C. G. Darwin, Proc. Roy. Soc. London, Ser. A 118, 654 (1928).⁶J. R. Shepard, E. Rost, and D. Murdock, Phys. Rev. Lett. 49, 14 (1982).⁷P. D. Kunz, DWUCK writeup (unpublished). For the nucleon bound state, the Dirac wave function is obtained iteratively with the strengths V_s and V_v adjusted by a factor to yield the separation energy.⁸R. C. Johnson and P. J. R. Soper, Phys. Rev. C 1, 976 (1970).⁹P. Schwandt *et al.*, to be published.¹⁰J. R. Shepard, E. Rost, and P. D. Kunz, Phys. Rev. C 25, 1127 (1982).¹¹D. W. Miller *et al.*, Bull. Am. Phys. Soc. 25, 522 (1980), and to be published.¹²C. Olmer *et al.*, to be published.¹³A. A. Rush *et al.*, Nucl. Phys. A104, 340 (1967); V. E. Lewis *et al.*, Nucl. Phys. A101, 589 (1967).¹⁴D. W. Miller *et al.*, Phys. Rev. C 20, 2008 (1979).

Determination of Relative Signs of Neutron and Proton Transition Matrix Elements: Strong Cancellation Observed for the $^{34}\text{S}(0^+ \rightarrow 2_2^+)$ Transition

A. M. Bernstein, R. A. Miskimen, B. Quinn, and S. A. Wood

Physics Department and Laboratory for Nuclear Science, Massachusetts Institute of Technology, Cambridge, Massachusetts 02139

and

M. V. Hynes

Los Alamos National Laboratory, Los Alamos, New Mexico 87545

and

G. S. Blanpied and B. G. Ritchie

University of South Carolina, Columbia, South Carolina 29208

and

V. R. Brown

Lawrence Livermore National Laboratory, Livermore, California 94550

(Received 25 May 1982)

Hadron scattering is shown to be sensitive to the relative sign of neutron and proton transition matrix elements. The relative signs for the 2_2^+ states are determined to be positive for ^{26}Mg , ^{30}Si , and ^{42}Ca , and negative for ^{34}S on the basis of proton differential cross-section measurements at 650 and 800 MeV. Suppression of the one-step amplitude in the ^{34}S 2_2^+ state causes the interference of one-step and multistep reactions to be experimentally apparent.

PACS numbers: 23.20.Js, 25.40.Ep, 27.30.+t, 27.40.+z

The sensitivity of inelastic hadron scattering (h, h') to both neutrons and protons offers the possibility of increasing our understanding of the neutron structure of nuclei by determining the relative signs of neutron and proton transition multipole matrix elements, M_n and M_p . In this Letter we present, for the first time, an example of hadronic measurements of these relative signs under conditions where the magnitudes (but not the signs) are previously known by electromagnetic (EM) methods.¹ This enables us to compare the experimental (h, h') results with predictions which sensitively depend on the relative sign of

 M_n and M_p .

A purely EM technique for obtaining the magnitudes of M_n and M_p using $B(E\lambda)$ values from mirror transition rates has been previously developed.¹ For a given analog transition one obtains $M_p(T_z)$ from $B(E\lambda, T_z; J_i \rightarrow J_f) = |M_p(T_z)|^2 / (2J_i + 1)$. To obtain $M_n(T_z)$ one uses the equivalent isospin representation for the matrix elements,

$$M_{n,p}(T_z) = [M_0(T_z) \pm M_1(T_z)] / 2, \quad (1)$$

where $M_0(T_z)$ and $M_1(T_z)$ are the isoscalar and isovector transition multipole matrix elements.

From charge independence M_0 is independent of